



CrossMark
click for updates

Cite this: *Chem. Sci.*, 2017, 8, 600

Carbon dioxide binding at a Ni/Fe center: synthesis and characterization of $\text{Ni}(\eta^1\text{-CO}_2\text{-}\kappa\text{C})$ and $\text{Ni-}\mu\text{-CO}_2\text{-}\kappa\text{C}:\kappa^2\text{O,O'}\text{-Fe}^\dagger$

Changho Yoo and Yunho Lee*

Received 3rd August 2016
Accepted 30th August 2016

DOI: 10.1039/c6sc03450k

www.rsc.org/chemicalscience

Introduction

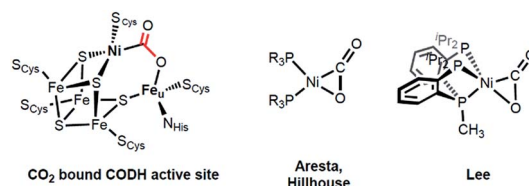
Activation of carbon dioxide is currently receiving much attention due to its relevance to environmental and energy related issues.¹ In the area of transition metal catalyzed reactions, one of the main challenges is selective reduction of CO_2 to a product such as formate, carbon monoxide, methanol or methane.² In a 2-electron process, the binding mode of the CO_2 may determine the eventual product formation, *e.g.* formate *vs.* carbon monoxide.³ When the initial metal–oxygen interaction occurs to form a metal CO_2 adduct $\text{M-}\eta^1\text{-CO}_2\text{-}\kappa\text{O}$, subsequent hydride transfer *via* CO_2 addition to a M-H bond generates a metal-formate species. Alternatively, the metal–carbon bond formation can produce a metallocarboxylate species ($\text{M-}\eta^1\text{-CO}_2\text{-}\kappa\text{C}$), followed by C–O bond cleavage to generate CO. In the latter case, an additional Lewis acid interaction can stabilize the negative charges at the oxygen atoms of the bound CO_2 .^{4,5} Therefore, CO_2 activation with a bimetallic system can be one way to guide the selectivity of the CO_2 catalyst and is receiving much attention.^{5,6} In fact, an excellent example of a bimetallic center utilized in an efficient catalytic conversion of CO_2 can be found in the active site of carbon monoxide dehydrogenase (CODH).⁷ According to recent studies, CO_2 coordination at a heterobimetallic nickel–iron active site can be found in CODH's intermediate species, which possesses a $\text{Ni-}\mu\text{-CO}_2\text{-Fe}$ moiety, Scheme 1.⁸ Although X-ray analysis provides a structural snapshot of the CO_2 reduction sequence, the role of the unique

iron ion is currently not well-understood.⁷ Thus, acquiring an understanding of iron assisted CO_2 –nickel coordination is of fundamental interest and is crucial for gaining mechanistic insight into this and other enzymatic reactions.

In organonickel chemistry, there are few mononuclear $\text{Ni-}\eta^2\text{-CO}_2$ adducts possessing both M–C and M–O bonds.⁹ In 1975, Aresta and co-workers reported the first structurally characterized nickel– CO_2 adduct $(\text{PCy}_3)_2\text{Ni}(\eta^2\text{-CO}_2)$, Scheme 1.^{9a} An analogous complex, $(\text{dtbpe})\text{Ni}(\eta^2\text{-CO}_2)$ (dtbpe = 1,2-bis(di-*tert*-butylphosphino)ethane) was recently reported by Hillhouse and co-workers.^{9d} More recently, our group reported a similar but unique five-coordinate nickel– CO_2 adduct $(\text{PP}^{\text{Me}}\text{P})\text{Ni}(\eta^2\text{-CO}_2)$ ($\text{PP}^{\text{Me}}\text{P}$ = $\text{PMe}(2\text{-P}^i\text{Pr}_2\text{-C}_6\text{H}_4)_2$).^{9f} According to its structural analysis, the five coordinate nickel CO_2 species supported by three neutral P donors has a weak Ni–O bond available for electrophilic attack.^{9f} Additionally, by utilizing an anionic tridentate PNP ligand ($\text{PNP}^- = \text{N}[2\text{-P}^i\text{Pr}_2\text{-4-Me-C}_6\text{H}_3]_2^-$), our group reported the nickel hydroxycarbonyl species $(\text{PNP})\text{NiCOOH}$ (1), $(\text{PNP})\text{NiCOONa}$ (2) and $\{(\text{PNP})\text{Ni}\}_2\text{-}\mu\text{-CO}_2\text{-}\kappa^2\text{C,O}$ (4), the first examples of $\text{Ni-}\text{CO}_2$ complexes that reveal a $\text{Ni-}\text{CO}_2\text{-}\kappa\text{C}$ binding mode, Scheme 2.¹⁰ The carboxylate group in these species is stabilized by a Lewis acid such as a proton, sodium or another nickel ion. Our interest then moved to comparing $(\text{PP}^{\text{Me}}\text{P})\text{Ni-}$

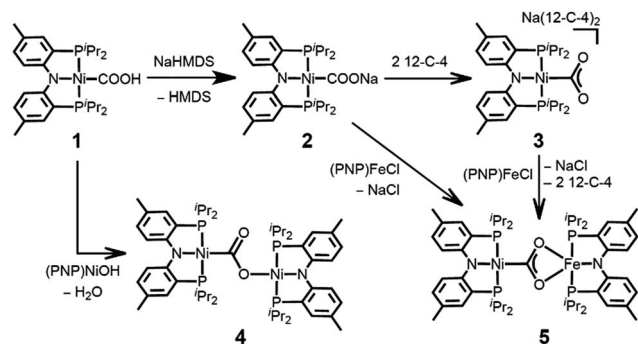
Department of Chemistry, Korea Advanced Institute of Science and Technology (KAIST), Daejeon 34141, Republic of Korea. E-mail: yunholee@kaist.ac.kr; Fax: +82 42 350 2810; Tel: +82 42 350 2814

† Electronic supplementary information (ESI) available: Characterization data for 3 and 5. CCDC 1492006 and 1492007. For ESI and crystallographic data in CIF or other electronic format see DOI: 10.1039/c6sc03450k



Scheme 1 The active site of carbon monoxide dehydrogenase (CODH, left), and 4- and 5-coordinate nickel CO_2 adducts (right).



Scheme 2 Preparation of mononuclear- and dinuclear- CO_2 adducts.

CO_2 and $(\text{PNP})\text{Ni}-\text{CO}_2$ to evaluate their fundamental differences in CO_2 activation. The different geometries favored with a $\text{PP}^{\text{Me}}\text{P}$ or PNP ligand affect the identity of the nickel- CO_2 moiety, which can be $\text{Ni}(\text{II})-\text{CO}_2^{2-}$ or $\text{Ni}(0)-\text{CO}_2$ or an open-shell $\text{Ni}(\text{I})-\text{CO}_2^{\cdot-}$, *vide infra*. Furthermore, by isolating the native nickel- CO_2 species, we can further study the effect of the second iron ion. Although several nickel carboxylate species are already known, iron has never been introduced synthetically into a $\text{Ni}-\text{CO}_2$ moiety.

Here, we present a nickel carboxylate species $\{\text{Na}(\text{12-C-4})_2\}\{(\text{PNP})\text{Ni}-\eta^1-\text{CO}_2-\kappa\text{C}\}$ (3), in which the nickel- CO_2 moiety does not have any Lewis acid interactions. We also prepared a dinuclear nickel-iron carboxylate species $(\text{PNP})\text{Ni}-\mu-\text{CO}_2-\kappa\text{C}:\kappa^2\text{O},\text{O}'-\text{Fe}(\text{PNP})$ (5), reminiscent of the NiFe -binuclear active site of CODH. This is an unprecedented example of a nickel-iron hetero-bimetallic complex possessing a bridging CO_2 ligand. The levels of CO_2 activation in compounds 3 and 5 are compared with other $\text{Ni}-\text{CO}_2$ adducts and the $\text{Ni}-\mu-\text{CO}_2-\text{Fe}$ moiety found in CODH.

Results and discussion

Synthesis and characterization of the $\text{Ni}-\eta^1-\text{CO}_2-\kappa\text{C}$ complex

The coordination of a hydroxycarbonyl moiety *via* a $\text{Ni}-\text{C}$ bond was previously realized at a divalent nickel center supported by a PNP ligand.¹⁰ Following deprotonation of $(\text{PNP})\text{NiCOOH}$ (1), its anionic congener $(\text{PNP})\text{NiCOONa}$ (2) was also prepared and recently reported by our group.¹⁰ The X-ray structure reveals that two molecules of 2 are oriented to form a pair with ionic interactions with two sodium ions in the crystal lattice, Fig. 1.¹¹ The corresponding CO_2 ligand coordinates to the nickel center in a $\mu_3-\kappa^1\text{C}:\kappa^2\text{O},\text{O}':\kappa^1\text{O}'$ mode with a $\text{Ni}-\text{C1}$ bond distance of 1.882(1) Å. There are additional bonds of the CO_2 moiety to sodium ions with $\text{Na}-\text{O}$ bond distances of 2.352(1), 2.217(1) and 2.459(1).¹¹ To obtain a sodium-free adduct, 2 equiv. of 12-crown-4 was added to a solution of 2, resulting in the formation of $\{\text{Na}(\text{12-C-4})_2\}\{(\text{PNP})\text{Ni}-\eta^1-\text{CO}_2-\kappa\text{C}\}$ (3). The crystal structure of 3 revealed the successful generation of a mononuclear nickel adduct possessing an $\eta^1-\kappa\text{C}$ coordinated carbon dioxide species with a $\text{Ni}-\text{C}$ bond distance of 1.911(2) Å, as shown in Fig. 1 and Table 1. The oxidation state of the nickel ion in 3 can be assigned as 2+ based on its similar structural features to

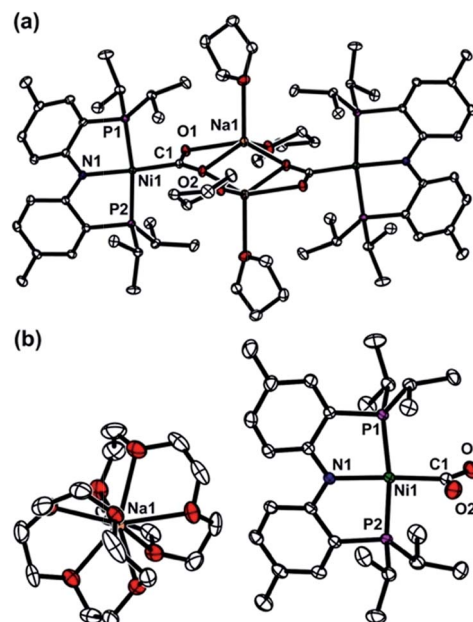


Fig. 1 Displacement ellipsoid (50%) representations for (a) $(\text{PNP})\text{NiCOONa}$ (2) in a dimeric assembly with co-crystallized THF molecules,¹¹ and (b) $\{\text{Na}(\text{12-C-4})_2\}\{(\text{PNP})\text{Ni}-\eta^1-\text{CO}_2-\kappa\text{C}\}$ (3). A co-crystallized 12-crown-4 molecule and hydrogen atoms are omitted for clarity.

previously known nickel(II) species such as $(\text{PNP})\text{NiCOOH}$ (1) and $\{(\text{PNP})\text{Ni}\}_2-\mu-\text{CO}_2-\kappa^2\text{C},\text{O}$ (4), *vide infra*. The geometry of 3 is square planar ($\tau_4 = 0.12^{12}$) with a similar but slightly elongated $\text{Ni}-\text{C}$ bond distance in comparison to those of 1 and 4 ($d_{\text{Ni}-\text{C}} = 1.866(2)$ and 1.888(2) Å, respectively, Table 1). This is probably due to a lower degree of π back-bonding between the nickel and CO_2 . In fact, π back-donation from the nickel center to a CO_2 ligand in such nickel carboxylate species is indicated by shorter $\text{Ni}-\text{C}$ distances (1.858–1.911 Å) than those of the nickel alkyl species $(\text{PNP})\text{NiR}$ ($\text{R} = \text{Me}, \text{Et}, \text{Pr}$) (1.963–2.004 Å).¹³ The molecular orbitals generated from DFT calculations also show the presence of π back-donation from the $\text{Ni } d_{xz}$ to the $\text{CO}_2 \pi^*$ orbital (see ESI†). Due to the absence of Lewis acid interactions in 3, a lower π -accepting ability of the CO_2 ligand is expected. Its structural data also revealed that the plane of the CO_2 ligand is perpendicular to that of the square planar $(\text{PNP})\text{Ni}$ moiety. One of the oxygen atoms ($d_{\text{Ni1}-\text{O2}} = 2.614(1)$ Å) is slightly closer to the nickel center than the other ($d_{\text{Ni1}-\text{O1}} = 2.776(1)$ Å), Table 2. These $\text{Ni}-\text{O}$ distances are much longer than those for other known $\text{Ni}-\eta^2-\text{CO}_2$ adducts (1.9–2.2 Å, Table 2), suggesting that neither of the oxygen atoms are bound.⁹ The DFT analysis also supports minimal interaction between the nickel and oxygen atoms (Wiberg index = 0.1358 for $\text{Ni1}-\text{O2}$ and 0.1679 for $\text{Ni1}-\text{O1}$, see Table 2). The two $\text{C}-\text{O}$ bond distances are nearly identical ($d_{\text{C1}-\text{O1}} = 1.247(2)$ Å, $d_{\text{C1}-\text{O2}} = 1.248(2)$ Å, Table 1) and slightly shorter than in the analogous carboxylate complexes 2 and 4 (Table 1), due to the absence of a Lewis acid, Na or Ni. According to the DFT analysis, the HOMO of 3 possesses contributions from both a nickel $d_{x^2-y^2}$ orbital and a $\text{CO}_2 \pi^*$ orbital, see Fig. 2. Due to additional electron density from



Table 1 Selected bond distances and angles for the nickel carboxylate species **1**, **2**, **3**, **4** and **5**, and CO₂-bound CODH

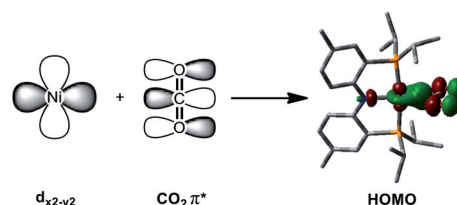
	1 ¹⁰	2 ¹¹	3	4 ¹⁰	5	CODH ^{8b}
<i>d</i> _{Ni-C} (Å)	1.866(2)	1.882(1)	1.911(2)	1.888(2)	1.858(1)	1.805(31)
<i>d</i> _{M-O} (Å)	—	2.352(1) ^a 2.217(1) ^a 2.459(1) ^a	—	1.897(2) ^b	2.204(1) ^c 2.066(1) ^c	2.030(18) ^c
<i>d</i> _{C-O} (Å)	1.269(3) 1.313(3)	1.260(1) 1.271(1)	1.247(2) 1.248(2)	1.240(3) 1.296(3)	1.269(2) 1.289(2)	1.298(30) 1.316(30)
Δ <i>d</i> _{C-O} (Å)	0.044	0.011	0.001	0.056	0.020	0.018
∠O-C-O (°)	119.6(2)	124.0(1)	128.4(2)	123.7(2)	116.5(1)	117.2(26)

^a M = Na. ^b M = Ni. ^c M = Fe.

CO₂²⁻ being shifted to the nickel, the CO₂ moiety is slightly oxidized compared to the sp² hybridized carboxylate ligands found in **2** and **4**. The larger O-C-O angle (128.4(2)°) of **3** compared to others (124.0(1) and 123.7(2)°) also supports this electronic feature, *vide infra*. Although an η¹-κC CO₂ coordination mode has been proposed for many CO₂ reduction strategies,^{2,3} the only example of a crystallographically identified metal η¹-κC CO₂ complex is a rhodium CO₂ adduct, Rh(CO₂)-(Cl)(diars)₂ (diars = *o*-phenylene-bis(dimethylarsine)), reported by the Herskovitz group.¹⁴ According to their C-O bond distances (1.20(2) and 1.25(2) Å) and O-C-O angle (126(2)°), the CO₂ moiety in **3** shares similar structural and electronic features. Thus, compound **3** is a unique example possessing η¹-κC CO₂ binding, since such a binding mode is unknown for 1st row transition metals and is rare in structurally characterized metal-CO₂ adducts.

Synthesis and characterization of the heterobimetallic nickel-iron CO₂ complex

To gain a better understanding of the role of the second metal ion in the CODH active site, we prepared a heterobimetallic nickel-iron carboxylate species possessing a Ni-CO₂-Fe

**Fig. 2** Combination of the Ni $d_{x^2-y^2}$ and CO₂ π^* orbitals provides the DFT calculated HOMO of {Na(12-C-4)₂}{(PNP)Ni-η¹-CO₂-κC} (**3**).

fragment by addition of {(PNP)Fe}⁺ to a Ni-η¹-CO₂-κC species. To a yellow solution of {Na(12-C-4)₂}{(PNP)Ni-η¹-CO₂-κC} (**3**) in toluene, a purple solution of (PNP)FeCl was added. The immediate formation of a new orange species (PNP)Ni-μ-CO₂-κC:κ²O,O'-Fe(PNP) (**5**) was confirmed, using the ¹H NMR spectrum, from the absence of peaks for **3** and (PNP)FeCl and the presence of new paramagnetically shifted signals. The same product was also prepared by substitution of the sodium ion of (PNP)NiCOONa (**2**) with (PNP)FeCl. The solid-state structure of **5** clearly revealed a dinuclear nickel-iron complex with a bridging CO₂ ligand in the μ₂-κC:κ²O,O' mode (Fig. 3). The Ni and Fe ions are separated by a distance of 4.3690(3) Å. The two C-O bond

Table 2 Selected physical parameters and bond indices from the natural bond orbital analysis

	Ni(PCy ₃) ₂ (η ² -CO ₂) ^{9a}	(dtbpe)Ni(η ² -CO ₂) ^{9d}	(PP ^{Me} P)Ni(η ² -CO ₂) ^{9f}	3	5
Structural parameters					
<i>d</i> _{Ni-C} (Å)	1.84(2)	1.868(2)	1.904(1)	1.911(2)	1.858(1)
<i>d</i> _{Ni-O} (Å)	1.99(2)	1.904(2)	2.191(1)	2.614(1) 2.776(1)	2.718(1) 2.792(1)
<i>d</i> _{C-O} (Å)	1.17(2) 1.22(2)	1.200(3) 1.266(3)	1.218(2) 1.252(2)	1.248(2) 1.247(2)	1.269(2) 1.289(2)
∠O-C-O (°)	133	138.0(2)	135.1(1)	128.4(2)	116.5(1)
ν _{CO₂} (cm ⁻¹)	1740	1724	1682	1620	1510
Wiberg bond indices^a					
Ni-C	—	0.5766	0.5286	0.6143	0.6277
Ni-O	—	0.4300	0.3117	0.1679 0.1358	0.0798 0.0644
C-O	—	1.6927 1.4080	1.6384 1.4701	1.5112 1.4949	1.3993 1.2933

^a Wiberg bond indices were calculated using single-point calculations, for which geometries were obtained from the XRD data.

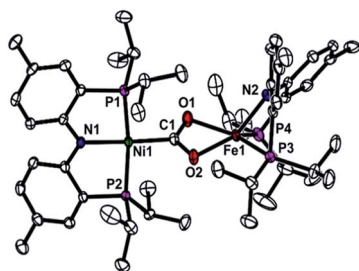


Fig. 3 Displacement ellipsoid (50%) representation for (PNP)Ni- μ -CO₂- κ C: κ^2 O, O' -Fe(PNP) (**5**). Hydrogen atoms are omitted for clarity.

distances are 1.269(2) and 1.289(2) Å, revealing that a significant elongation has occurred due to the iron interaction compared to **3** (Table 1). The bond distances between the iron and both oxygen atoms are 2.204(1) and 2.066(1) Å. The nickel center possesses a square planar geometry ($\tau_4 = 0.10^{12}$). The geometry around the iron is distorted square pyramidal ($\tau = 0.13$,¹⁵ Fig. 3). The O1–C1–O2 angle (116.5°) reflects the sp^2 hybridization of the carboxylate ligand in **5**. In fact, recent crystallographic data of CODH at atomic resolution ($d_{\min} = 1.03$ Å) revealed that the bound CO₂ molecule ($\angle O-C-O = 117.2(26)^\circ$) is a carboxylate anion (CO₂²⁻).^{8b,8c} Regarding the similarity between these angles, the carboxylate moiety in **5** might be close to CO₂²⁻. The asymmetric vibration for CO₂ observed at 1510 cm⁻¹, which is similar to that observed for the dinickel carboxylate species (**4**) at 1518 cm⁻¹, also indicates a reduced state of CO₂. The effective magnetic moment of **5** was determined using the Evans' method ($\mu_{\text{eff}} = 4.95 \mu_B$ in C₆D₆), which indicated an $S = 2$ spin state.¹⁶ According to DFT calculations, most of the spin density is located on the iron center (see ESI†). For CODH, the unique iron, Fe_u, was assigned as a high spin iron(II) (ferrous component II, FCII) using Mössbauer spectroscopy,¹⁷ and a low-spin nickel(II) was demonstrated using X-ray absorption spectroscopy (XAS).¹⁸ The current structural and spectroscopic analyses suggest that **5** might share a similar electronic structure to that found in CODH. Gibson classified the μ_2 - κ C: κ^2 O, O' binding modes of CO₂ into two types according to the difference between the two C–O distances.¹⁹ Due to the two similar C–O distances of the CO₂ moiety, compound **5** ($\Delta d_{C-O} = 0.020$ Å) can be assigned as a class I complex.²⁰ In the dinickel CO₂ species (**4**), the CO₂ molecule is coordinated in a μ_2 - κ C: κ O mode with the absence of a Ni2–O2 interaction ($d_{\text{Ni2-O2}} = 3.14(7)$) and two different C–O bond distances ($\Delta d_{C-O} = 0.056$ Å). In CODH, CO₂ is coordinated in a μ_2 - κ C: κ O fashion between the nickel and iron ions, but the two C–O bond distances are quite comparable ($\Delta d_{C-O} = 0.018$ Å), akin to the μ_2 - κ C: κ^2 O, O' mode. This might be due to hydrogen bonding with the protein matrix, since both the CO₂ oxygens are hydrogen bonded to His93 and Lys563, respectively.⁸

Compound **5** is the first example of a dinuclear nickel–iron–CO₂ complex. While dinuclear CO₂ complexes mostly employ 2nd and 3rd row transition metals,¹⁹ several bimetallic iron carboxylates (Fe–CO₂–M, M = Ti, Zr, Sn, Re) have been reported.^{5a,5c–e,21} However, such complexes typically possess an Fe–C bond rather than an Fe–O bond with CO₂. There have been

numerous examples of nickel–iron bimetallic complexes reported for synthetic model studies of NiFe hydrogenase,²² but a bimetallic complex possessing a Ni- μ -CO₂-Fe moiety closely related to CODH chemistry is not known. The Holm group constructed a series of [NiFe₃S₄] cubanes as structural model complexes for the [NiFe₄S₄] core in CODH.²³ However, the installation of an iron species corresponding to the Fe_u in CODH and reactions involving CO and CO₂ have not yet been investigated. More recently, the Holm group also reported a bimetallic complex containing nickel and iron supported by a binucleating macrocycle.²⁴ With respect to CODH chemistry, bridging hydoroxy, cyanido and formato species have been generated, however, a Ni- μ -CO₂-Fe fragment had not yet been isolated.

Activation of CO₂ in **3** and **5**

Previously known 4-coordinate Ni–CO₂ complexes possessing an η^2 -CO₂ binding mode have a formally zero-valent nickel center, Scheme 1.⁹ This suggests limited CO₂ activation in such species. Interestingly, the 5-coordinate nickel CO₂ adduct (PP^{Me}P)Ni(CO₂) also has a similar level of activation of CO₂ based on the C–O bond distances and the O–C–O angle, Table 2. Regarding CO₂ binding and activation, {Na(12-C-4)}{(PNP)Ni- η^1 -CO₂- κ C} (**3**) is a unique example. It is striking that a neutral pincer-type ligand PP^{Me}P (PP^{Me}P = PMe[2-PⁱPr₂-C₆H₄]₂) favors 5-coordinate η^2 -CO₂ coordination at a single nickel center, while **3** remains as a 4-coordinate species with η^1 -CO₂ coordination.^{9f} Although the total number of Ni d-electrons and CO₂ π^* -electrons in both **3** and (PP^{Me}P)Ni(CO₂) is the same, (PP^{Me}P)Ni(CO₂) can be considered as formally Ni(0)–(CO₂) while **3** can be better described as a Ni(II)–(CO₂²⁻) species. The asymmetric CO₂ stretching frequency for **3** is significantly shifted to a lower vibration, 1620 cm⁻¹, compared to those of the Ni- η^2 -CO₂ complexes (Table 2), which is evidence of a reduced CO₂ moiety in **3**.⁹ This may be due to the influence of the *trans* atom: an anionic amide nitrogen *vs.* a neutral phosphorus atom. The anionic nitrogen in **3** electrostatically favors a divalent nickel center, while the neutral π -acidic P atom in the PP^{Me}P ligand favors a Ni(0) center. In fact, the PNP ligand typically stabilizes a square planar geometry while the PP^{Me}P ligand favors a pseudo-tetrahedral geometry. Thus, **3** prefers to accommodate a divalent nickel center while (PP^{Me}P)Ni(CO₂) prefers Ni(0). However, the reduction state of the CO₂ moiety in **3** is a little ambiguous according to the O–C–O angle. The O–C–O angle in **3** of 128.4(2)° is larger than those of an ideal sp^2 hybridized carbon (120°) and the other nickel(II) carboxylate species **1**, **2** and **4** (119.6(2)°, 124.0(1)° and 123.7(2)°, respectively, Table 1). The O–C–O angle of a CO₂ radical anion (CO₂^{•-}) is suggested to be 133°,²⁵ which is fairly similar to those of the previously reported Ni- η^2 -CO₂ complexes, Table 2. Thus, the geometry of the CO₂ moiety in **3** may be thought of as being between a CO₂ radical anion and a carboxylate.

Upon addition of iron to compound **3**, the CO₂ is further reduced to carboxylate (CO₂²⁻). The C–O bond distances and O–C–O angle in **5** clearly show a 2-electron reduced state of the CO₂ moiety, Table 2. This was also indicated by the asymmetric CO₂



vibration observed at 1510 cm^{-1} , which is significantly lower than those of other CO_2 species and **3**. The Wiberg bond indices nicely agree with the bond distances, Table 2. These analyses of a series of nickel- CO_2 compounds demonstrate how the degree of CO_2 activation can be tuned by incorporating a distinct electronic coordination environment at the metal center, and may have parallels to the efficient CO_2 conversion found in CODH.

In order to study further activation of the bound CO_2 via C–O bond cleavage, protonation of **3** and **5** was attempted. Our group previously reported that reversible C–O bond cleavage/formation occurs with a nickel hydroxycarbonyl species (**1**).¹⁰ From reaction of **3** with 1 equiv. of $\text{HBF}_4 \cdot \text{Et}_2\text{O}$, a nickel hydroxycarbonyl species (**1**) was produced and isolated with a 74% yield. A similar reaction of **3** with 2 equiv. of $\text{HBF}_4 \cdot \text{Et}_2\text{O}$ resulted in the formation of a carbonyl species $\{(\text{PNP})\text{NiCO}\}\{\text{BF}_4\}$ in 75% yield, revealing that two sequential protonations can occur with compound **3** possessing a $\text{Ni}-\eta^1\text{-CO}_2-\kappa\text{C}$ moiety, which are key steps in the transformation of CO_2 to CO. Although protonation of compound **5** seems to produce **1** and $\{(\text{PNP})\text{NiCO}\}\{\text{BF}_4\}$, unfortunately, their yields were not clear due to thermal decomposition of **5** and the generation of multiple products. Demetallation of the iron seems to be one of the decomposition processes.

Conclusions

In conclusion, the generation of unprecedented nickel-carbon dioxide adducts possessing a Ni–C bond accommodated by a (PNP)Ni scaffold was accomplished. A mononuclear CO_2 adduct $\{\text{Na}(\text{12-C-4})_2\}\{(\text{PNP})\text{Ni}-\eta^1\text{-CO}_2-\kappa\text{C}\}$ (**3**) and a dinuclear nickel-iron carboxylate species $(\text{PNP})\text{Ni}-\mu\text{-CO}_2-\kappa\text{C}:\kappa^2\text{O},\text{O}'\text{-Fe}(\text{PNP})$ (**5**) were synthesized successfully. While the solid state structure of **3** revealed a rare $\eta^1\text{-}\kappa\text{C}$ binding mode, compound **5** was structurally characterized to reveal a unique class I type $\mu_2\text{-}\kappa\text{C}:\kappa^2\text{O},\text{O}'$ binding mode. This heterobimetallic CO_2 adduct is the first example of a nickel-iron carboxylate species, of which the structural and electronic features are reminiscent of those of the $\text{Ni}-\mu\text{-CO}_2\text{-Fe}$ fragment found in the C-cluster of CODH. Comparison of the $\eta^1\text{-CO}_2-\kappa\text{C}$ species **3** and dinuclear $\text{Ni}-\mu\text{-CO}_2\text{-Fe}$ species **5** with previously reported $\text{Ni}-\text{CO}_2$ adducts suggested that the CO_2 ligand can be stabilized and activated by interaction with the second metal. Protonation of **3** produces a nickel carbonyl species $\{(\text{PNP})\text{NiCO}\}\{\text{BF}_4\}$ via C–O bond cleavage, while the reactivity of **5** is limited. Further studies on incorporating a stable iron species and the subsequent reactivity toward protonation are currently underway.

Acknowledgements

This work was supported by the C1 Gas Refinery Program (NRF-2015M3D3A1A01064880) through the National Research Foundation of Korea (NRF-2015R1A2A2A01004197), and KAIST and the Aramco Overseas Company. This work was also supported by the Supercomputer Center/Korea Institute of Science and Technology (KSC-2015-S1-0005).

Notes and references

- (a) Q. Liu, L. Wu, R. Jackstell and M. Beller, *Nat. Commun.*, 2015, **6**, 5933; (b) M. Aresta, A. Dibenedetto and A. Angelini, *Chem. Rev.*, 2014, **114**, 1709; (c) M. Aresta, *Carbon Dioxide as Chemical Feedstock*, Wiley-VCH, Weinheim, 2010.
- (a) J. Qiao, Y. Liu, F. Hong and J. Zhang, *Chem. Soc. Rev.*, 2014, **43**, 631; (b) C. Finn, S. Schnittger, L. J. Yellowlees and J. B. Love, *Chem. Commun.*, 2012, **48**, 1392; (c) E. Fujita, *Coord. Chem. Rev.*, 1999, **185–186**, 373.
- (a) J. Song, E. L. Klein, F. Neese and S. Ye, *Inorg. Chem.*, 2014, **53**, 7500; (b) M. R. Dubois and D. L. Dubois, *Acc. Chem. Res.*, 2009, **42**, 1974; (c) E. E. Benson, C. P. Kubiak, A. J. Sathrum and J. M. Smieja, *Chem. Soc. Rev.*, 2009, **38**, 89.
- (a) M. Devillard, R. Declercq, E. Nicolas, A. W. Ehlers, J. Backs, N. Saffon-Merceron, G. Bouhadir, J. C. Slootweg, W. Uhl and D. Bourissou, *J. Am. Chem. Soc.*, 2016, **138**, 4917; (b) S. J. K. Forrest, J. Clifton, N. Fey, P. G. Pringle, H. A. Sparkes and D. F. Wass, *Angew. Chem., Int. Ed.*, 2015, **54**, 2223.
- (a) M. Hirano, M. Akita, K. Tani, K. Kumagai, N. C. Kasuga, A. Fukuoka and S. Komiyama, *Organometallics*, 1997, **16**, 4206; (b) K. E. Litz, K. Henderson, R. W. Gourley and M. M. B. Holl, *Organometallics*, 1995, **14**, 5008; (c) J. R. Pinkes, B. D. Steffey, J. C. Vites and A. R. Cutler, *Organometallics*, 1994, **13**, 21; (d) J. R. Pinkes and A. R. Cutler, *Inorg. Chem.*, 1994, **33**, 759; (e) J. C. Vites, B. D. Steffey, M. E. Giuseppetti-Dery and A. R. Cutler, *Organometallics*, 1991, **10**, 2827; (f) E. G. Lundquist, J. C. Huffman, K. Folting, B. E. Mann and K. G. Caulton, *Inorg. Chem.*, 1990, **29**, 128; (g) E. G. Lundquist, J. C. Huffman and K. G. Caulton, *J. Am. Chem. Soc.*, 1986, **108**, 8309; (h) S. Gambarotta, F. Arena, C. Floriani and P. F. Zanazzi, *J. Am. Chem. Soc.*, 1982, **104**, 5082; (i) G. Fachinetti, C. Floriani and P. F. Zanazzi, *J. Am. Chem. Soc.*, 1978, **100**, 7405.
- (a) C. W. Machan and C. P. Kubiak, *Dalton Trans.*, 2016, DOI: 10.1039/C6DT01956K, in press; (b) S. Bagherzadeh and N. P. Mankad, *J. Am. Chem. Soc.*, 2015, **137**, 10898; (c) O. Cooper, C. Camp, J. Pécaut, C. E. Kefalidis, L. Maron, S. Gambarelli and M. Mazzanti, *J. Am. Chem. Soc.*, 2014, **136**, 6716; (d) J. P. Krogman, B. M. Foxman and C. M. Thomas, *J. Am. Chem. Soc.*, 2011, **133**, 14582; (e) B. D. Steffey, C. J. Curtis and D. L. DuBois, *Organometallics*, 1995, **14**, 4937.
- M. Can, F. A. Armstrong and S. W. Ragsdale, *Chem. Rev.*, 2014, **114**, 4149.
- (a) J.-H. Jeoung and H. Dobbek, *Science*, 2007, **318**, 1461; (b) J. Fessler, J.-H. Jeoung and H. Dobbek, *Angew. Chem., Int. Ed.*, 2015, **54**, 8560; (c) M. W. Ribbe, *Angew. Chem., Int. Ed.*, 2015, **54**, 8337.
- (a) M. Aresta, C. F. Nobile, V. G. Albano, E. Forni and M. Manassero, *J. Chem. Soc., Chem. Commun.*, 1975, 636; (b) M. Aresta and C. F. Nobile, *J. Chem. Soc., Dalton Trans.*, 1977, 708; (c) A. Döhring, P. W. Jolly, C. Krüger and



- M. J. Romão, *Z. Naturforsch., B: J. Chem. Sci.*, 1985, **40**, 484; (d) J. S. Anderson, V. M. Iluc and G. L. Hillhouse, *Inorg. Chem.*, 2010, **49**, 10203; (e) R. Beck, M. Shoshani, J. Krasinkiewicz, J. A. Hatnean and S. A. Johnson, *Dalton Trans.*, 2013, **42**, 1461; (f) Y.-E. Kim, J. Kim and Y. Lee, *Chem. Commun.*, 2014, **50**, 11458.
- 10 C. Yoo, J. Kim and Y. Lee, *Organometallics*, 2013, **32**, 7195.
- 11 C. Yoo and Y. Lee, *Inorg. Chem. Front.*, 2016, **3**, 849.
- 12 L. Yang, D. R. Powell and R. P. Houser, *Dalton Trans.*, 2007, 955.
- 13 C. Yoo, S. Oh, J. Kim and Y. Lee, *Chem. Sci.*, 2014, **5**, 3853.
- 14 J. C. Calabrese, T. Herskovitz and J. B. Kinney, *J. Am. Chem. Soc.*, 1983, **105**, 5914.
- 15 A. W. Addison, T. N. Rao, J. Reedijk, J. van Rijn and G. C. Verschoor, *J. Chem. Soc., Dalton Trans.*, 1984, 1349.
- 16 (a) D. F. Evans, *J. Chem. Soc.*, 1959, 2003; (b) S. K. Sur, *J. Magn. Reson.*, 1989, **82**, 169.
- 17 Z. Hu, N. J. Spangler, M. E. Anderson, J. Xia, P. W. Ludden, P. A. Lindahl and E. Münck, *J. Am. Chem. Soc.*, 1996, **118**, 830.
- 18 W. Gu, J. Seravalli, S. W. Ragsdale and S. P. Cramer, *Biochemistry*, 2004, **43**, 9029.
- 19 D. H. Gibson, *Chem. Rev.*, 1996, **96**, 2063.
- 20 Classification of the $\mu_2\text{-}\kappa\text{C}:\kappa^2\text{O},\text{O}'$ binding modes of CO_2 for a bimetallic center (M and M'): while the CO_2 coordinates *via* a M–C bond, class I complexes have the two oxygen atoms of the CO_2 ligand symmetrically bonded to M' and class II complexes possess two asymmetric M'–O bonds.
- 21 (a) D. H. Gibson, J. F. Richardson and T.-S. Ong, *Acta Crystallogr., Sect. C: Cryst. Struct. Commun.*, 1991, **47**, 259; (b) D. H. Gibson, M. Ye and J. F. Richardson, *J. Am. Chem. Soc.*, 1992, **114**, 9716; (c) D. H. Gibson, J. F. Richardson and O. P. Mbadike, *Acta Crystallogr., Sect. B: Struct. Sci.*, 1993, **49**, 784; (d) D. H. Gibson, M. Ye, J. F. Richardson and M. S. Mashuta, *Organometallics*, 1994, **13**, 4559; (e) D. H. Gibson, M. Ye, B. A. Sleadd, J. M. Mehta, O. P. Mbadike, J. F. Richardson and M. S. Mashuta, *Organometallics*, 1995, **14**, 1242; (f) M. Lutz, M. Haukka, T. A. Pakkanen and L. H. Gade, *Organometallics*, 2001, **20**, 2631.
- 22 (a) S. Kaur-Ghumaan and M. Stein, *Dalton Trans.*, 2014, **43**, 9392; (b) A. C. Marr, D. J. E. Spencer and M. Schröder, *Coord. Chem. Rev.*, 2001, **219–221**, 1055.
- 23 (a) S. Ciurli, P. K. Ross, M. J. Scott, S.-B. Yu and R. H. Holm, *J. Am. Chem. Soc.*, 1992, **114**, 5415; (b) R. Panda, C. P. Berlinguette, Y. Zhang and R. H. Holm, *J. Am. Chem. Soc.*, 2005, **127**, 11092; (c) J. Sun, C. Tessier and R. H. Holm, *Inorg. Chem.*, 2007, **46**, 2691.
- 24 D. Huang and R. H. Holm, *J. Am. Chem. Soc.*, 2010, **132**, 4693.
- 25 (a) D. W. Ovenall and D. H. Whiffen, *Mol. Phys.*, 1961, **4**, 135; (b) J. W. Rabalais, J. M. McDonald, V. Scherr and S. P. McGlynn, *Chem. Rev.*, 1971, **71**, 73.

